

Title	EVAPORATION AND CONDENSATION OF A RAREFIED GAS BETWEEN ITS TWO PARALLEL PLANE CONDENSED PHASES WITH DIFFERENT TEMPERATURES AND NEGATIVE TEMPERATURE-GRADIENT PHENOMENON : NUMERICAL ANALYSIS OF THE BOLTZMANN EQUATION FOR HARD-SPHERE MOLECULES(Mathematical Analysis of Fluid and Plasma Dynamics)
Author(s)	Sone, Yoshio; Ohwada, Taku; Aoki, Kazuo
Citation	数理解析研究所講究録 (1990), 734: 106-122
Issue Date	1990-12
URL	<a href="http://hdl.handle.net/2433/102005">http://hdl.handle.net/2433/102005</a>
Right	
Type	Departmental Bulletin Paper
Textversion	publisher

EVAPORATION AND CONDENSATION OF A RAREFIED GAS BETWEEN ITS TWO  
PARALLEL PLANE CONDENSED PHASES WITH DIFFERENT TEMPERATURES  
AND NEGATIVE TEMPERATURE-GRADIENT PHENOMENON  
— NUMERICAL ANALYSIS OF THE BOLTZMANN EQUATION  
FOR HARD-SPHERE MOLECULES —

Yoshio Sone, Taku Ohwada, and Kazuo Aoki  
Department of Aeronautical Engineering  
Kyoto University, Kyoto 606, Japan

曾根良夫, 大和田拓, 青木一生 (京大・工)

A rarefied gas between its two parallel plane condensed phases is considered, and its steady behavior, especially the rate of evaporation or condensation on the condensed phases and the negative temperature-gradient phenomenon, is studied numerically on the basis of the linearized Boltzmann equation for hard-sphere molecules under the conventional boundary condition and its generalization. The method of analysis is the finite-difference method developed recently by the authors. Not only the temperature and density distributions and the mass and energy fluxes in the gas but also the velocity distribution function of the gas molecules is obtained with good accuracy for the whole range of the Knudsen number.

## I. INTRODUCTION

Consider a rarefied gas between its two parallel plane condensed phases with different temperatures. The gas evaporates on the condensed phase with higher temperature and condenses on the other. This simple and fundamental problem of evaporation and condensation draws special attention in connection with the negative temperature-gradient phenomenon.<sup>1-9</sup> The analyses of the problem are, however, based on the Boltzmann-Krook-Welander (BKW) equation or crude assumptions. Thus, its accurate analysis on the basis of the standard Boltzmann equation is required but has not yet been carried out because of the complex collision integral in the Boltzmann equation.

In this paper we try to carry out the accurate analysis of this two-surface problem of evaporation and condensation for the whole range of the Knudsen number on the basis of the linearized Boltzmann equation for hard-sphere molecules. The method used in the analysis is the finite-difference method developed in the temperature-jump problem by the authors,<sup>10</sup> where an efficient way of computation of the linearized collision integral is proposed and its universal numerical data useful for

analyzing various problems are stored. We first consider the problem under the conventional boundary condition on the condensed phase specified in Sec. II, for which the velocity distribution function of the molecules leaving the condensed phase is independent of that of the incident molecules. Then, we discuss the problem under a generalized boundary condition suggested by the experiment by Wortberg<sup>9</sup> and show that the solution for the generalized condition is derived from that for the conventional condition by simple formulae.

## II. PROBLEM AND ASSUMPTION

Consider a rarefied gas between its two parallel infinite plane condensed phases at rest with different temperatures. Let the temperature of one of the condensed phases [at  $X_1 = -D/2$ , ( $D > 0$ );  $X_1$  is the rectangular space coordinate system] be  $T_0(1 - \Delta\tau)$  and that of the other (at  $X_1 = D/2$ ) be  $T_0(1 + \Delta\tau)$ . We investigate the steady behavior of the gas (the velocity distribution function, the temperature and density distributions, and the mass and energy fluxes in the gas) for the whole range of the Knudsen number (the mean free path of the gas molecules divided by the distance between the condensed phases  $D$ ) under the following assumptions:

- (i) The gas molecules are hard spheres of a uniform size and undergo complete elastic collisions between themselves, and the behavior of the gas is described by the Boltzmann equation.
- (ii) In Secs. III - V, we consider the problem under the conventional boundary condition on each condensed phase. That is, the gas molecules leaving each condensed phase constitute the corresponding part of the Maxwellian distribution pertaining to the stationary saturated gas at the temperature [ $T_0(1 + \Delta\tau)$  or  $T_0(1 - \Delta\tau)$ ] of the condensed phase. In Sec. VI, we discuss the extension of the solution to the problem under a more general boundary condition.
- (iii) The difference of the temperatures of the condensed phases is so small ( $|\Delta\tau| \ll 1$ ) that the governing equation and boundary condition can be linearized around a uniform equilibrium state at rest.

We summarize the remaining main notations used in this paper:  $\rho_0$  is the saturation gas density at temperature  $T_0$ ;  $p_0 = R\rho_0 T_0$  (the saturation pressure at  $T_0$ );  $R$  is the specific gas constant (the Boltzmann constant divided by the mass of a molecule);  $\ell_0$  is the mean free path of the gas molecules at the saturated equilibrium state at rest with temperature  $T_0$ ;  $Kn = \ell_0/D$  (the Knudsen number);  $k = (\sqrt{\pi}/2)Kn$ ;  $x_1 = X_1/D$ ;  $(2RT_0)^{1/2}\xi_1$  is the molecular velocity;  $\xi = (\xi_1^2)^{1/2}$ ;  $E(\xi) = \pi^{-3/2}\exp(-\xi^2)$ ;  $\rho_0(2RT_0)^{-3/2}E(\xi)(1 + \phi)$  is the velocity distribution function of the gas molecules;  $\rho_0(1 + \omega)$  is the density of the gas;  $T_0(1 + \tau)$  is the gas

temperature;  $p_0(1 + P)$  is the gas pressure;  $(2RT_0)^{1/2}u_i$  is the flow velocity;  $p_0(\delta_{ij} + P_{ij})$  is the stress tensor ( $\delta_{ij}$  is Kronecker's delta);  $p_0(2RT_0)^{1/2}Q_i$  is the heat flow vector;  $p_0(2RT_0)^{1/2}H_i$  is the energy flow vector. Further, the saturation gas pressure at temperature  $T_0(1 + \Delta\tau)$  is assumed to be given by  $p_0(1 + \beta\Delta\tau)$ , where  $\beta$  is a positive constant corresponding to the slope of the Clausius-Clapeyron curve at  $T_0$ .

### III. BASIC EQUATION

The linearized Boltzmann equation for a steady state in the present spatially one-dimensional case is<sup>11</sup>

$$\xi_1 \frac{\partial \phi}{\partial x_1} = \frac{1}{k} [L_1(\phi) - L_2(\phi) - \nu(\xi)\phi], \quad (1)$$

$$L_1(\phi) = \frac{1}{\sqrt{2\pi}} \int \frac{1}{|\xi_1 - \xi_i|} \exp(-\xi_i^2 + \frac{|\xi_i \wedge \xi_1|^2}{|\xi_1 - \xi_i|^2}) \phi(x_1, \xi_i) d\vec{\xi}, \quad (2a)$$

$$L_2(\phi) = \frac{1}{2\sqrt{2\pi}} \int |\xi_1 - \xi_i| \exp(-\xi_i^2) \phi(x_1, \xi_i) d\vec{\xi}, \quad (2b)$$

$$\nu(\xi) = \frac{1}{2\sqrt{2}} [\exp(-\xi^2) + (2\xi + \frac{1}{\xi}) \int_0^\xi \exp(-c^2) dc], \quad (2c)$$

where  $\xi_i$  is the variable of integration corresponding to  $\xi_1$ ,  $\xi_i \wedge \xi_1$  is the vector product of  $\xi_i$  and  $\xi_1$ ,  $d\vec{\xi} = d\xi_1 d\xi_2 d\xi_3$ , and the domain of integration in  $L_1$ ,  $L_2$ , and all the following integrals with respect to the molecular velocity ( $\xi_i$  or  $\xi_1$ ) is the whole molecular velocity space unless otherwise stated.

The boundary condition for Eq. (1) on the condensed phases ( $x_1 = \pm 1/2$ ) is given as

$$\phi(1/2, \xi_1) = (\beta + \xi_1^2 - \frac{5}{2})\Delta\tau, \quad (\xi_1 < 0), \quad (3a)$$

$$\phi(-1/2, \xi_1) = -(\beta + \xi_1^2 - \frac{5}{2})\Delta\tau, \quad (\xi_1 > 0). \quad (3b)$$

The solution of the boundary-value problem (1), (3a), and (3b) exists uniquely.<sup>12</sup> From the uniqueness theorem and symmetry of Eqs. (1) - (3b), the solution satisfies

$$\phi(x_1, \xi_1, \xi_2, \xi_3) = -\phi(-x_1, -\xi_1, \xi_2, \xi_3), \quad (4)$$

especially the reflection condition at  $x_1 = 0$ :

$$\phi(0, \xi_1, \xi_2, \xi_3) = -\phi(0, -\xi_1, \xi_2, \xi_3). \quad (5)$$

Further, in the same way as in Ref. 10, we can show that the solution takes the form

$$\phi = \phi(x_1, \xi_1, \xi_r), \quad \xi_r = (\xi_2^2 + \xi_3^2)^{1/2}. \quad (6)$$

Thus, the number of the independent variables is reduced to three.

The nondimensional macroscopic variables,  $\omega$ ,  $\tau$ ,  $u_i$ , etc., are given as the moments of  $\phi$ :

$$\begin{aligned} \omega &= \int \phi \text{Ed}\vec{\xi}, & u_1 &= \int \xi_1 \phi \text{Ed}\vec{\xi}, \\ \tau &= \frac{2}{3} \int (\xi^2 - \frac{3}{2}) \phi \text{Ed}\vec{\xi}, & P &= \omega + \tau, \\ P_{1j} &= 2 \int \xi_1 \xi_j \phi \text{Ed}\vec{\xi}, & Q_1 &= \int \xi_1 \xi^2 \phi \text{Ed}\vec{\xi} - \frac{5}{2} u_1, \\ H_1 &= \int \xi_1 \xi^2 \phi \text{Ed}\vec{\xi} = Q_1 + \frac{5}{2} u_1. \end{aligned} \quad (7)$$

From the conservation equations which are derived from Eq. (1) by multiplying it by 1,  $\xi_1$ , or  $\xi^2$  and integrating the result over the whole molecular velocity space, we have

$$u_1 = \text{const}, \quad P_{11} = 0, \quad Q_1 = \text{const}, \quad H_1 = \text{const}, \quad (8)$$

where Eq. (5) is used for the second equation. These equations will be used for the accuracy test of our numerical computation.

The dependence of the solution on the parameters  $\beta$  and  $\Delta\tau$  is very simple. That is, if the solutions for two special values of  $\beta$ , say  $\beta_1$  and  $\beta_2$ , are known, then the solution for an arbitrary  $\beta$  is given by

$$\phi(\beta=\beta) = \frac{\Delta\tau}{\beta_1 - \beta_2} [(\beta - \beta_2)\phi(\beta=\beta_1, \Delta\tau=1) + (\beta_1 - \beta)\phi(\beta=\beta_2, \Delta\tau=1)]. \quad (9)$$

#### IV. NUMERICAL ANALYSIS

The boundary-value problem (1), (3a), and (5) over the domain ( $0 \leq x_1 \leq 1/2$ ) is quite similar to that treated in Ref. 10 [cf. Eqs. (20), (21), and (23) there]. Thus, we can readily make use of the method, scheme, and stored data of computation in Ref. 10.

We determine the solution of the boundary-value problem by pursuing the long-time behavior of the solution of the initial and boundary-value problem [Eq. (1) with the additional  $\partial\phi/\partial t$  term on the left-hand side, boundary condition (3a) and (5), and an initial condition (e.g.,  $\phi = 0$ )].

The time-dependent problem is solved numerically by a finite-difference method. The finite-difference scheme for the differential operator is a standard implicit one [cf. Eqs. (33), (34a), and (34b) in Ref. 10]. In the collision integral, the velocity distribution function  $\phi E$  is expanded in terms of a system of basis functions such as used in the finite element method. The basis functions are chosen in such a way that  $\phi E$  is approximated by a sectionally quadratic function of  $\xi_1$  and  $\xi_r$  that takes the exact value at the lattice points in  $(\xi_1, \xi_r)$  [cf. Appendix A in Ref. 10]. Thus the collision integral is expressed by the product of the collision integral matrix ( $D_{jklm}$  in Ref. 10) and the column vector consisting of the values of  $\phi E$  at the lattice points. The collision integral matrix is the collision integral of the basis functions ( $\Psi_{lm}$  in Ref. 10) at the lattice points and thus is a universal matrix. We have built the matrix for three lattice systems of different fineness in Refs. 10 and 13. Thus, we can effectively compute the collision integral not only for the present problem but also for any problem where the molecular velocity dependence of  $\phi E$  is  $\xi_1$  and  $\xi_r$  only. Further, the present method of computation is very convenient to vectorize the program of computation for a vector computer such as FACOM VP-400E.

In our finite difference computation, the space interval  $0 \leq x_1 \leq 1/2$  is divided into 100 sections, uniform for  $k \geq 1$ , and nonuniform for  $k < 1$  with the minimum width 0.0005 ( $k = 0.1$ )  $\sim$  0.004 ( $k = 0.8$ ) around  $x_1 = 1/2$  and the maximum width 0.0183 ( $k = 0.1$ )  $\sim$  0.00795 ( $k = 0.8$ ) around  $x_1 = 0$ . The  $\xi_1 \xi_r$  space is limited to the finite region ( $-4.429 \leq \xi_1 \leq 4.429$ ,  $0 \leq \xi_r \leq 4$ ), and the region is divided into 36 uniform sections for  $\xi_r$  and 116 nonuniform sections for  $\xi_1$  with the minimum width 0.0036 around  $\xi_1 = 0$  and the maximum width 0.2182 around  $\xi_1 = \pm 4.429$ . Thus, there are 4329 lattice points in  $\xi_1 \xi_r$  space. This lattice system for  $\xi_1 \xi_r$  is finer than that used in Ref. 10 and is called M3 in Ref. 13. The limitation of  $\xi_1$  and  $\xi_r$  to the finite region is legitimate in view of the form of Eqs. (1) - (3), (5), and (7), where the interaction terms of different molecular velocities are multiplied by rapidly decaying functions, and it is confirmed by the computation.

## V. RESULT OF ANALYSIS

The temperature and density distributions in the gas are shown in Tables I and II and Figs. 1a, b, and c, where  $\omega$  and  $-\tau$  (or  $-\omega$  and  $\tau$ ) are drawn so that the pressure  $P$  can be easily read as the difference (or distance) of the two curves. For large  $\beta$ , the temperature gradient in the center region of the gas is in the opposite direction to that of the maintained temperature gradient between the two condensed phases. The possibility of the inverse temperature gradient, called negative temperature-gradient phenomenon, was first noted in the limit  $k \rightarrow 0$  and

has been discussed by various authors.<sup>1-8</sup> Its physical mechanism is discussed in Ref. 2; its thermodynamic discussion is given in Ref. 7. In the limit  $k \rightarrow 0$ , the inverse temperature gradient occurs when

$$\begin{aligned} \beta &> 4.6992, & (\text{hard sphere}), \\ &> 4.7723, & (\text{BKW}), \end{aligned} \quad (10)$$

which is derived by the asymptotic theory of the Boltzmann equation for small Knudsen numbers.<sup>2,10,13-16</sup> The  $\beta$  at the onset of the inverse temperature gradient,  $\beta_{rT}$ , for general  $k$  is given in Table III. In the free molecular flow ( $k = \infty$ ), the temperature is uniform ( $\tau = 0$ ) irrespective of  $\beta$ .

The gas velocity  $u_1$ , heat flow  $Q_1$ , and energy flow  $H_1$  versus  $k$  are shown for  $\beta = 2$  and 12 in Fig. 2 and Table III. The results for arbitrary  $\beta$  are easily obtained by the same linear combination as in Eq. (9). The mass and energy flows are always from the hotter condensed phase to the colder, but a heat flow in the opposite direction is observed for large  $\beta$ . For large  $\beta$ ,  $-H_1$  takes its minimum at an intermediate Knudsen number, and around  $\beta = 2 \sim 3$ , so does  $-u_1$ . The value of  $\beta$  for which the reversal of the direction of the heat flow occurs is also tabulated as  $\beta_{rQ}$  in Table III. It does not depend much on the Knudsen number. The asymptotic results for small  $k$  can be obtained with the aid of the asymptotic theory:<sup>2,10,13,16</sup>

$$\begin{aligned} u_1 &= - \frac{c_1 \beta + (c_2 + c_3 \beta)k}{1 + c_0 k} \Delta\tau, & Q_1 &= - \frac{5}{2} k \frac{(1 + c_4 \beta)k}{1 + c_0 k} \Delta\tau, \\ H_1 &= - \frac{5}{2} \frac{c_1 \beta + [c_5 + c_6 \beta]k}{1 + c_0 k} \Delta\tau, & \beta_{rT} = \beta_{rQ} &= - c_4^{-1}, \end{aligned} \quad (11)$$

$$\begin{aligned} c_0 &= 4.3327, & c_1 &= 0.4670, & c_2 &= -1.0224, & c_3 &= 2.2411, & c_4 &= -0.2128, \\ (c_4^{-1} &= -4.6992), & \kappa &= 1.922284, & c_5 &= c_2 + \kappa, & c_6 &= \kappa c_4 + c_3, \end{aligned}$$

where all the terms of the asymptotic series are taken. They are also shown in Fig. 2 and Table III. The onset of the inverse heat flow generally differs from that of the inverse temperature gradient but agrees with it in the limit  $k \rightarrow 0$ .

The velocity distribution functions  $\phi E$  at three points in the gas are shown for  $k = 0.1, 1, \text{ and } 10$  and for  $\beta = 2, 12, \text{ and } \beta_{rQ}$  in Figs. 3 - 5. For a given  $\beta$ , the velocity distribution function  $\phi E / \Delta\tau$  for  $\xi_1 < 0$  at  $x_1 = 0.5$  takes the same form for any  $k$  [cf. Eq. (3a)]. Thus these are good examples to see the effect of molecular collisions. For large  $k$ , the variation of  $\phi E$  with respect to  $x_1$  is small except around  $\xi_1 = 0$ , where the collision effect is localized, and the variation with respect to  $\xi_1$  is

very steep around  $\xi_1 = 0$ .

## VI. GENERAL BOUNDARY CONDITION

So far we discussed the problem under the conventional boundary condition on the condensed phase, where the velocity distribution function of the molecules leaving the condensed phase is determined by the condition of the condensed phase and is independent of the velocity distribution of the molecules incident on the condensed phase. The generalized boundary condition suggested by Wortberg's experiment<sup>9</sup> showing the dependence of the distribution of the leaving molecules on that of the incident molecules on a solid surface is given as follows. The velocity distribution of the leaving molecules is given by the sum of two terms:  $\alpha_c$  times of the distribution stated in (ii) of Sec. II and  $(1 - \alpha_c)$  times of the diffuse reflection distribution<sup>17</sup>, where  $\alpha_c$  ( $0 \leq \alpha_c \leq 1$ ) is a constant called condensation factor. In the present problem, from Eqs. (3a) and (3b) and Eq. (3) in Ref. 18, it is given by

$$\phi = (\bar{\beta}_+ + \xi^2 - \frac{5}{2})\Delta\tau, \quad (\xi_1 < 0, x_1 = \frac{1}{2}), \quad (12a)$$

$$\bar{\beta}_+ = \alpha_c \beta + (1 - \alpha_c) \left[ \frac{1}{2} + 2\sqrt{\pi}(\Delta\tau)^{-1} \int_{\xi_1 > 0} \xi_1 \phi\left(\frac{1}{2}, \xi_1\right) \text{Ed}\xi \right],$$

$$\phi = -(\bar{\beta}_- + \xi^2 - \frac{5}{2})\Delta\tau, \quad (\xi_1 > 0, x_1 = -\frac{1}{2}), \quad (12b)$$

$$\bar{\beta}_- = \alpha_c \beta + (1 - \alpha_c) \left[ \frac{1}{2} + 2\sqrt{\pi}(\Delta\tau)^{-1} \int_{\xi_1 < 0} \xi_1 \phi\left(-\frac{1}{2}, \xi_1\right) \text{Ed}\xi \right].$$

The conventional condition corresponds to  $\alpha_c = 1$ , and the diffuse reflection boundary condition without evaporation and condensation corresponds to  $\alpha_c = 0$ . The latter problem was treated in Ref. 18.

Under the assumption that  $\alpha_c$  takes a common value on both the condensed phases, the solution of Eqs. (1), (12a), and (12b) is easily seen to have the symmetry of Eqs. (4) and (5). Thus

$$\bar{\beta}_+ = \bar{\beta}_- = \bar{\beta}. \quad (13)$$

Noting the symmetry and comparing Eqs. (12a) and (12b) with Eqs. (3a) and (3b), we find that the solution under the generalized boundary condition is expressed by the solution under the conventional condition with different  $\beta$ . That is, let  $\phi(x_1, \xi_1; \beta)$  be the solution under Eqs. (3a) and (3b), and  $\phi_\alpha(x_1, \xi_1; \beta_\alpha)$  the solution under Eqs. (12a) and (12b) with a different  $\beta$  (i.e.,  $\beta = \beta_\alpha$ ) and the same  $k$ . Then the relation between  $(\beta, \phi)$  and  $(\beta_\alpha, \phi_\alpha)$  is given by



$$\beta_{\alpha} = \frac{\beta}{\alpha_c} - \frac{1 - \alpha_c}{\alpha_c} \left[ \frac{1}{2} + 2\sqrt{\pi}(\Delta\tau)^{-1} \int_{\xi_1 > 0} \xi_1 \phi\left(\frac{1}{2}, \xi_1; \beta\right) \text{Erd}\xi \right], \quad (14)$$

$$\phi_{\alpha}(x_1, \xi_1; \beta_{\alpha}) = \phi(x_1, \xi_1; \beta). \quad (15)$$

In view of Eq. (9), the quantity in the square brackets of Eq. (14) is a linear function of  $\beta$ . That is,

$$[*] = a(k)\beta + b(k), \quad (16)$$

where  $a(k)$  and  $b(k)$  are given in Table III. The  $\beta_{\alpha}$  increases as  $\alpha_c$  decreases when  $\beta > b(k)/[1 - a(k)]$ . In Table III,  $b(k)/[1 - a(k)] < 1$ . For  $\beta_{\alpha}$  given by Eq. (14), the same state as that under the conventional boundary condition is realized under the generalized boundary condition. Thus the inverse temperature gradient or the inverse heat flow is also found under the generalized boundary condition.

Making use of Eq. (9) to eliminate  $\phi$  and  $\beta$  from Eqs. (14) and (15), we have the solution for arbitrary  $\alpha_c$  ( $\neq 0$ ) and  $\beta_{\alpha}$  in terms of two solutions with different  $\beta$ ,  $\beta_1$  and  $\beta_2$ , under the conventional condition as

$$\phi_{\alpha}(\beta = \beta_{\alpha}) = \frac{1}{\beta_1 - \beta_2} [(A\beta_{\alpha} + B - \beta_2)\phi(\beta = \beta_1) - (A\beta_{\alpha} + B - \beta_1)\phi(\beta = \beta_2)], \quad (17)$$

$$A = \frac{\alpha_c}{1 - a(k)(1 - \alpha_c)}, \quad B = \frac{b(k)(1 - \alpha_c)}{1 - a(k)(1 - \alpha_c)}. \quad (18)$$

We can, therefore, obtain the necessary data for an arbitrary  $\alpha_c$  from those given in Sec. V.

From the point of solving the problem, the solution for all the cases including  $\alpha_c = 0$  is obtained by a linear combination of the solutions of two boundary value problems, say Eqs. (1), (5), and (19a) below and Eqs. (1), (5), and (19b) below.

$$\phi = 1, \quad (\xi_1 < 0, \quad x_1 = \frac{1}{2}), \quad (19a)$$

$$\phi = \xi^2, \quad (\xi_1 < 0, \quad x_1 = \frac{1}{2}). \quad (19b)$$

In the present work, we obtain the data from the solutions say,  $\Phi_1$  and  $\Phi_2$  of the two boundary-value problems, Eqs. (1), (5), and (19a) and Eqs. (1), (5), and (19b). That is,

$$\phi_{\alpha}(\beta = \beta_{\alpha})(\Delta\tau)^{-1} = (A\beta_{\alpha} + B - \frac{5}{2})\Phi_1 + \Phi_2. \quad (20)$$

For smaller  $k$  the numerical error in the collision integral is more important to the solution. This effect for small  $k$  can be reduced by solving the problem in two steps: i) solve  $\Phi_J$  ( $J = 1$  or  $2$ ) and compute corresponding  $u_1$ . ii) consider  $\tilde{\Phi}_J$ :

$$\tilde{\Phi}_J = \Phi_J(\text{new}) - 2\xi_1 u_1(\text{old}), \quad (21)$$

where  $\Phi_J(\text{new})$  is the final solution  $\Phi_J$  to be solved and  $u_1(\text{old})$  is the preliminary  $u_1$  solved in the first step; derive the equation and boundary condition for  $\tilde{\Phi}_J$ ; and then solve  $\tilde{\Phi}_J$ , from which  $\Phi_J(\text{new})$  is obtained.

As the accuracy test of our numerical computation, we examine the constancy of  $u_1$ ,  $P_{11}$ , and  $H_1$  [Eq. (8)] for  $\Phi_1$  and  $\Phi_2$ . The results are:

$$\begin{aligned} V(u_1) < 3.6 \times 10^{-5}, \quad |P_{11}| < 5.4 \times 10^{-5}, \quad V(H_1) < 2.2 \times 10^{-4}, \\ V(u_1) = \max(u_1(x_1)) - \min(u_1(x_1)), \quad (\text{for each } \Phi_J \text{ and } k). \end{aligned} \quad (22)$$

The computation was carried out by FACOM VP-400E at the Data Processing Center, Kyoto University.

#### REFERENCES

1. Y. P. Pao, *Phys. Fluids* **14**, 306 (1971).
2. Y. Sone and Y. Onishi, *J. Phys. Soc. Jpn.* **44**, 1981 (1978).
3. L. D. Koffman, M. S. Plesset, and L. Lees, *Phys. Fluids* **27**, 876 (1984).
4. T. Matsushita, *Phys. Fluids* **19**, 1712 (1976).
5. P. N. Shankar and M. D. Deshpande, *Pramāṇa - J. Phys.* **31**, L337 (1988).
6. T. Ytrehus and T. Aukrust, in *Rarefied Gas Dynamics*, edited by V. Boffi and C. Cercignani (Teubner, Stuttgart, 1986), Vol. 2, p. 271.
7. L. J. F. Hermans and J. J. M. Beenakker, *Phys. Fluids* **29**, 4231 (1986).
8. K. Aoki and C. Cercignani, *Phys. Fluids* **26**, 1163 (1983).
9. R. Mager, G. Adomeit, and G. Wortberg, in *Rarefied Gas Dynamics*, edited by D. P. Weaver, E. P. Muntz, and D. H. Campbell (AIAA, New York, 1989) (to be published).
10. Y. Sone, T. Ohwada, and K. Aoki, *Phys. Fluids A* **1**, 363 (1989).
11. H. Grad, in *Rarefied Gas Dynamics*, edited by J. A. Laurmann (Academic, New York, 1963), p. 26.
12. C. Cercignani, *J. Math. Phys.* **8**, 1653 (1967).
13. Y. Sone, T. Ohwada, and K. Aoki, *Phys. Fluids A* **1** (1989) (to be published).
14. Y. Sone, in *Rarefied Gas Dynamics*, edited by L. Trilling and H. Y. Wachman (Academic, New York, 1969), p. 243.
15. Y. Sone, in *Rarefied Gas Dynamics*, edited by D. Dini (Editrice Tecnico Scientifica, Pisa, 1971), p. 737.
16. Y. Sone and K. Aoki, *Transp. Theory Stat. Phys.* **16**, 189 (1987); *Mem. Fac. Eng. Kyoto Univ.* **49**, 237 (1987).
17. C. Cercignani, *The Boltzmann Equation and Its Applications* (Springer, Berlin, 1987).
18. T. Ohwada, K. Aoki, and Y. Sone, in *Rarefied Gas Dynamics*, edited by D. P. Weaver, E. P. Muntz, and D. H. Campbell (AIAA, New York, 1989) (to be published).



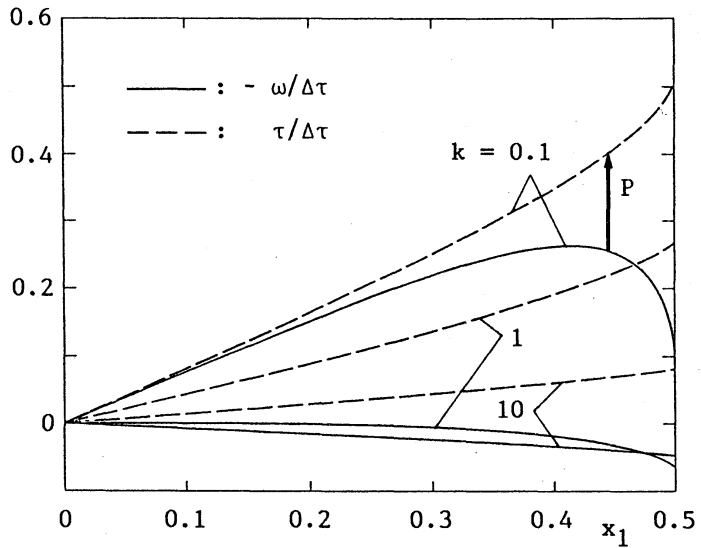


Table III.  $u_1$ ,  $Q_1$ ,  $H_1$ ,  $\beta_{rT}$ ,  $\beta_{rQ}$ ,  $a(k)$ , and  $b(k)$ .

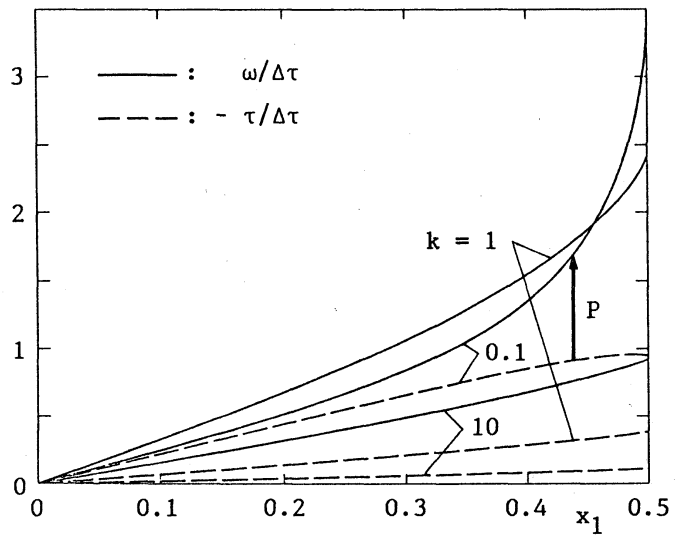
k	$\beta = 2$				$\beta = 12$				$\beta_{rT}$	$\beta_{rQ}$	a(k)	b(k)
	$u_1/\Delta\tau$	$Q_1/\Delta\tau$	$H_1/\Delta\tau$	$H_1/\Delta\tau$	$u_1/\Delta\tau$	$Q_1/\Delta\tau$	$H_1/\Delta\tau$	$H_1/\Delta\tau$				
$\infty$	-0.8463	-0.7052	-2.821	-2.821	-6.488	2.116	-14.10	-14.10	—	4.5	-1	1
20.00	-0.8428	-0.6908	-2.798	-2.798	-6.425	2.046	-14.02	-14.02	6.185	4.524	-0.9789	0.9702
15.00	-0.8419	-0.6864	-2.791	-2.791	-6.408	2.026	-13.99	-13.99	6.204	4.530	-0.9730	0.9616
10.00	-0.8404	-0.6779	-2.779	-2.779	-6.376	1.990	-13.95	-13.95	6.227	4.541	-0.9625	0.9456
8.00	-0.8395	-0.6719	-2.771	-2.771	-6.355	1.965	-13.92	-13.92	6.235	4.549	-0.9553	0.9346
6.00	-0.8383	-0.6624	-2.758	-2.758	-6.324	1.926	-13.88	-13.88	6.237	4.559	-0.9446	0.9175
4.00	-0.8366	-0.6448	-2.736	-2.736	-6.271	1.858	-13.82	-13.82	6.219	4.576	-0.9264	0.8872
3.00	-0.8356	-0.6288	-2.718	-2.718	-6.227	1.799	-13.77	-13.77	6.187	4.590	-0.9113	0.8606
2.00	-0.8348	-0.6003	-2.687	-2.687	-6.158	1.700	-13.70	-13.70	6.109	4.610	-0.8872	0.8152
1.50	-0.8350	-0.5753	-2.663	-2.663	-6.106	1.617	-13.65	-13.65	6.025	4.625	-0.8684	0.7770
1.00	-0.8369	-0.5328	-2.625	-2.625	-6.029	1.482	-13.59	-13.59	5.863	4.644	-0.8406	0.7143
0.80	-0.8391	-0.5058	-2.603	-2.603	-5.987	1.400	-13.57	-13.57	5.752	4.654	-0.8250	0.6755
0.60	-0.8432	-0.4672	-2.575	-2.575	-5.936	1.286	-13.55	-13.55	5.590	4.665	-0.8052	0.6214
0.40	-0.8516	-0.4069	-2.536	-2.536	-5.869	1.113	-13.56	-13.56	5.334	4.678	-0.7787	0.5387
0.30	-0.8592	-0.3613	-2.509	-2.509	-5.828	0.9844	-13.59	-13.59	5.148	4.685	-0.7615	0.4771
0.20	-0.8716	-0.2960	-2.475	-2.475	-5.780	0.8034	-13.65	-13.65	4.914	4.692	-0.7399	0.3898
	(-0.8711)	-0.2958	-2.474	-2.474	(-5.774)	0.8000	-13.64	-13.64	(4.6992)	4.6992	(-0.7382)	0.3884
0.15	-0.8808	-0.2510	-2.453	-2.453	-5.751	0.6800	-13.70	-13.70	4.788	4.696	-0.7263	0.3301
	(-0.8806)	-0.2510	-2.453	-2.453	(-5.749)	0.6788	-13.69	-13.69	(4.6992)	4.6992	(-0.7257)	0.3295
0.10	-0.8931	-0.1926	-2.425	-2.425	-5.716	0.5211	-13.77	-13.77	4.692	4.698	-0.7095	0.2531
	(-0.8930)	-0.1926	-2.425	-2.425	(-5.715)	0.5209	-13.77	-13.77	(4.6992)	4.6992	(-0.7094)	0.2529
0.08	-0.8991	-0.1640	-2.412	-2.412	-5.698	0.4436	-13.80	-13.80	(4.6992)	4.6992	(-0.7014)	0.2153
0.06	-0.9060	-0.1314	-2.397	-2.397	-5.678	0.3555	-13.84	-13.84	(4.6992)	4.6992	(-0.6923)	0.1726
0.04	-0.9140	-0.0941	-2.379	-2.379	-5.658	0.2545	-13.89	-13.89	(4.6992)	4.6992	(-0.6818)	0.1236
0.02	-0.9232	-0.0508	-2.359	-2.359	-5.633	0.1374	-13.95	-13.95	(4.6992)	4.6992	(-0.6698)	0.0667
0.01	-0.9284	-0.0265	-2.347	-2.347	-5.619	0.0716	-13.98	-13.98	(4.6992)	4.6992	(-0.6629)	0.0347
0.00	-0.9340	0.0000	-2.335	-2.335	(-5.604)	0.0000	-14.01	-14.01	(4.6992)	4.6992	(-0.6556)	0.0000

\* The data in the parentheses are obtained by the asymptotic theory<sup>10,13,16</sup> [cf. Eq. (11)].

(a)  $\beta = 2$



(b)  $\beta = 12$



(c)  $\beta = \beta_{rT}$  :

$$\beta_{rT} = \begin{cases} 4.692 & (k=0.1) \\ 5.863 & (k=1) \\ 6.227 & (k=10) \end{cases}$$

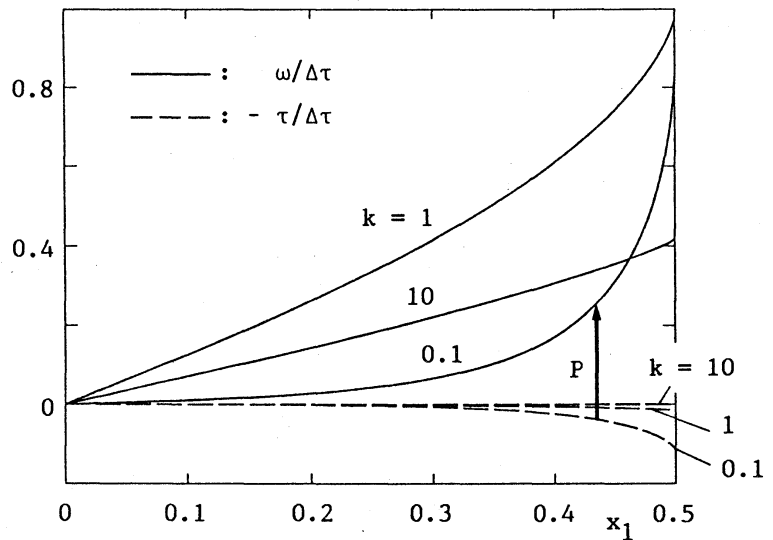


Fig. 1. Temperature and density distributions.

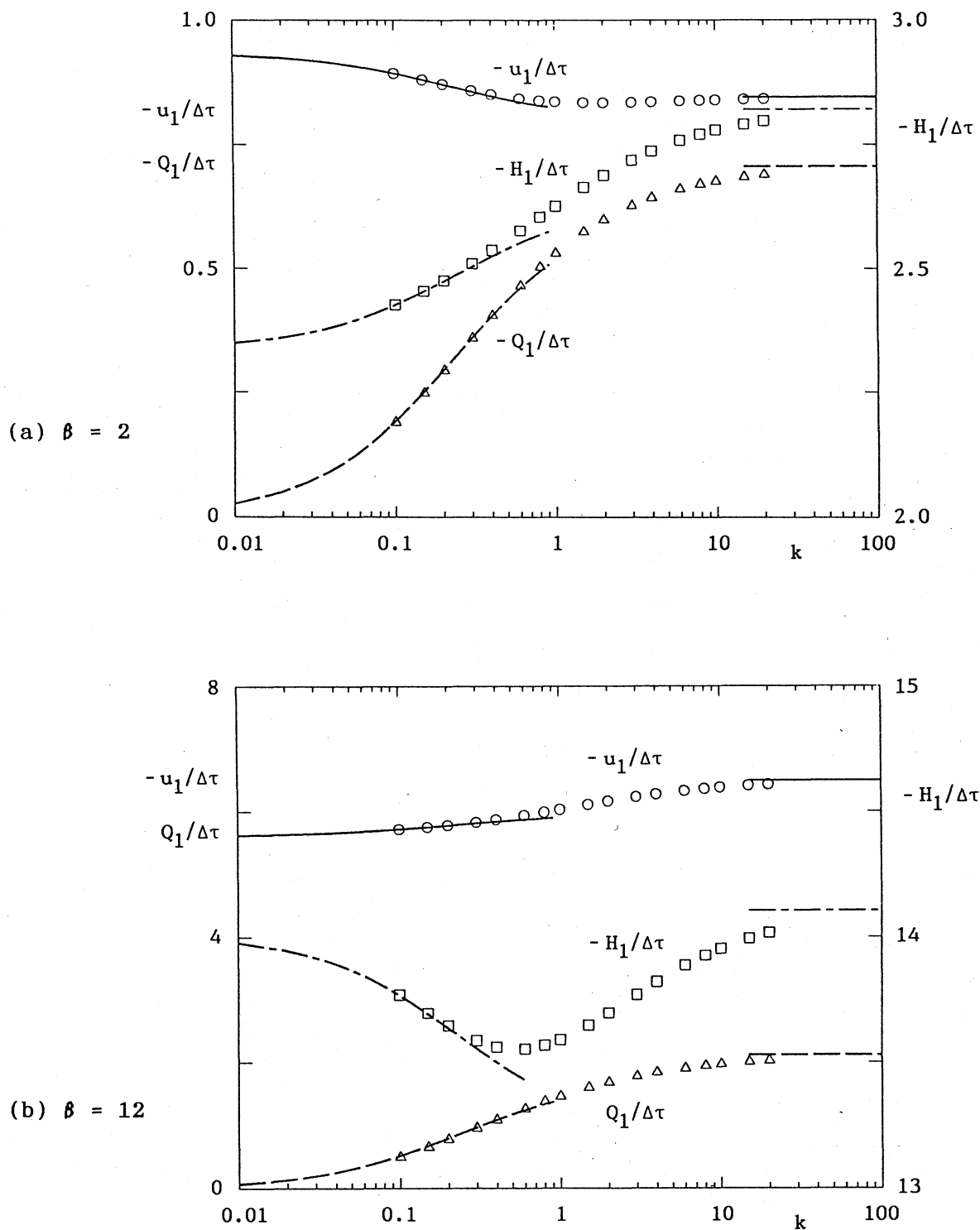


Fig. 2.  $u_1$ ,  $Q_1$ , and  $H_1$ .  $\circ$ ,  $\Delta$ , and  $\square$  indicate the numerical results. The curves for small  $k$  indicate the analytical results [Eq. (11)] by the asymptotic theory<sup>10,13,16</sup>. The straight lines for large  $k$  indicate the results for the free molecular flow.

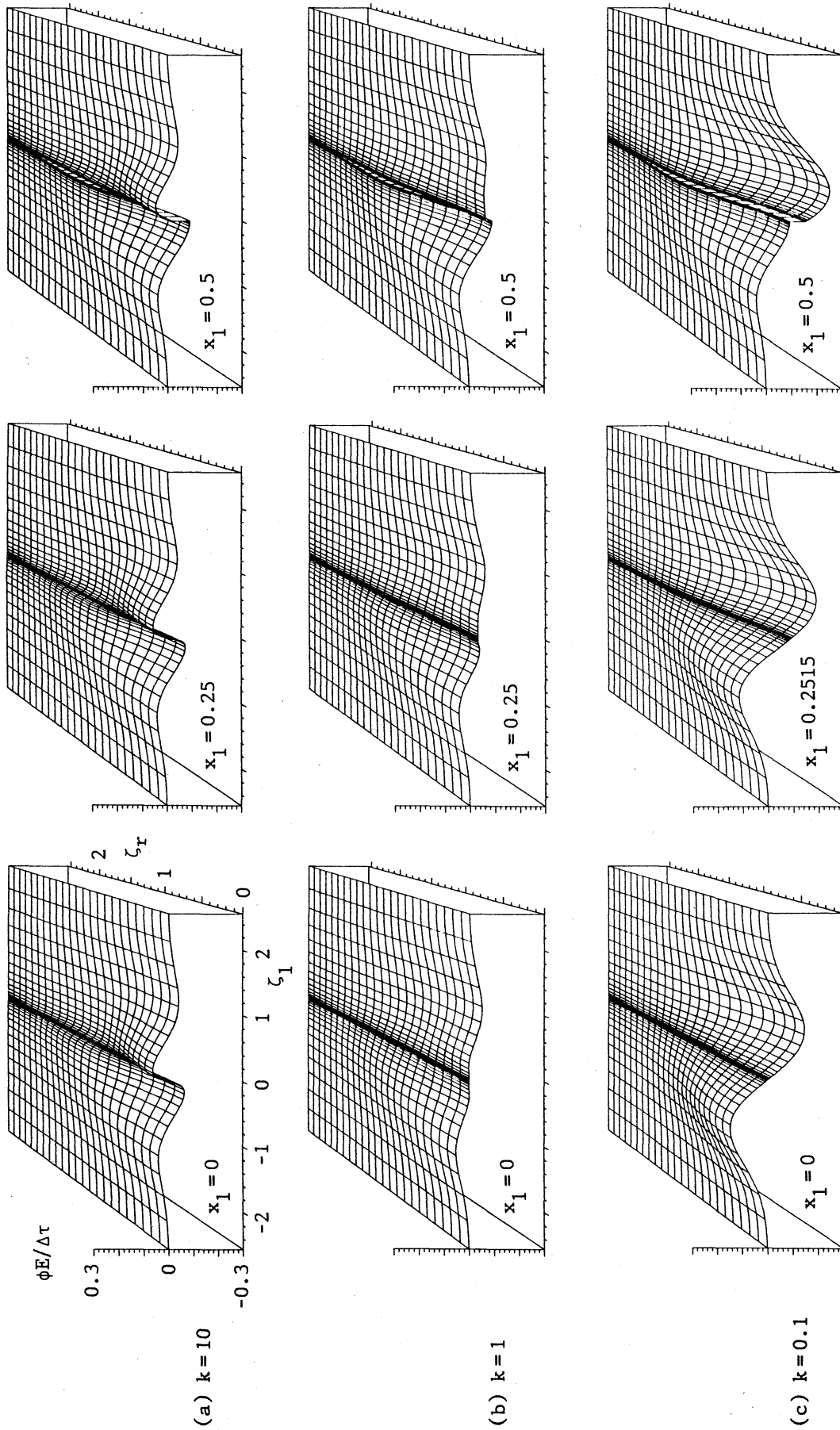


Fig. 3. The velocity distribution function  $\phi E$  ( $\beta=2$ ). The scales are common for all the figures. Each three  $\zeta_1 = \text{const}$  and each  $\zeta_r = \text{const}$  lattices in our computation are shown on the surface  $\phi E / \Delta \tau$ . The  $\phi E / \Delta \tau$  is negligibly small at the four corners in the figures, and therefore they may be taken as the reference points.



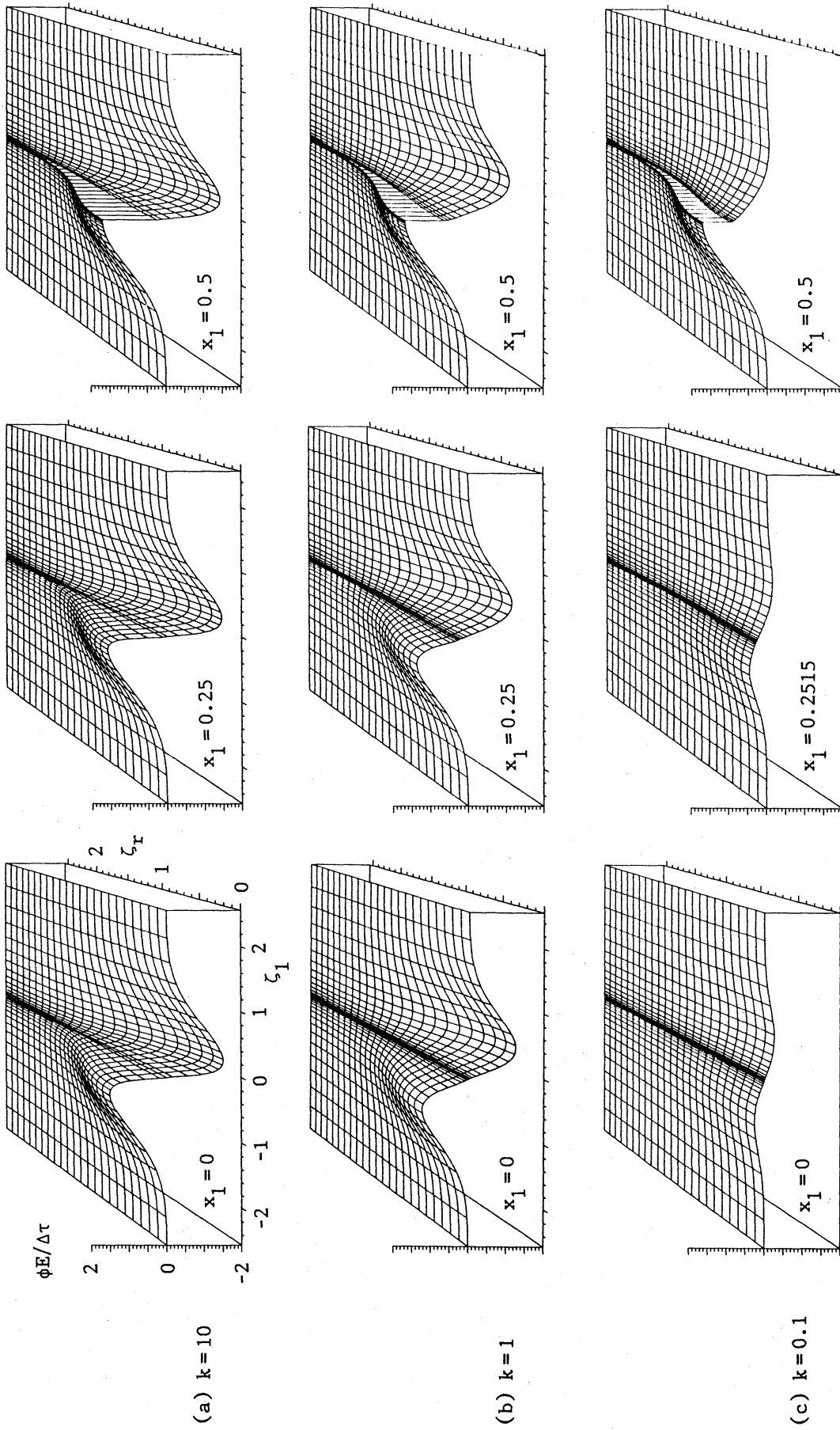


Fig. 4. The velocity distribution function  $\phi E$  ( $\beta=12$ ). The scales are common for all the figures. Each three  $\zeta_1 = \text{const}$  and each  $\zeta_r = \text{const}$  lattices in our computation are shown on the surface  $\phi E / \Delta \tau$ . The  $\phi E / \Delta \tau$  is negligibly small at the four corners in the figures, and therefore they may be taken as the reference points.

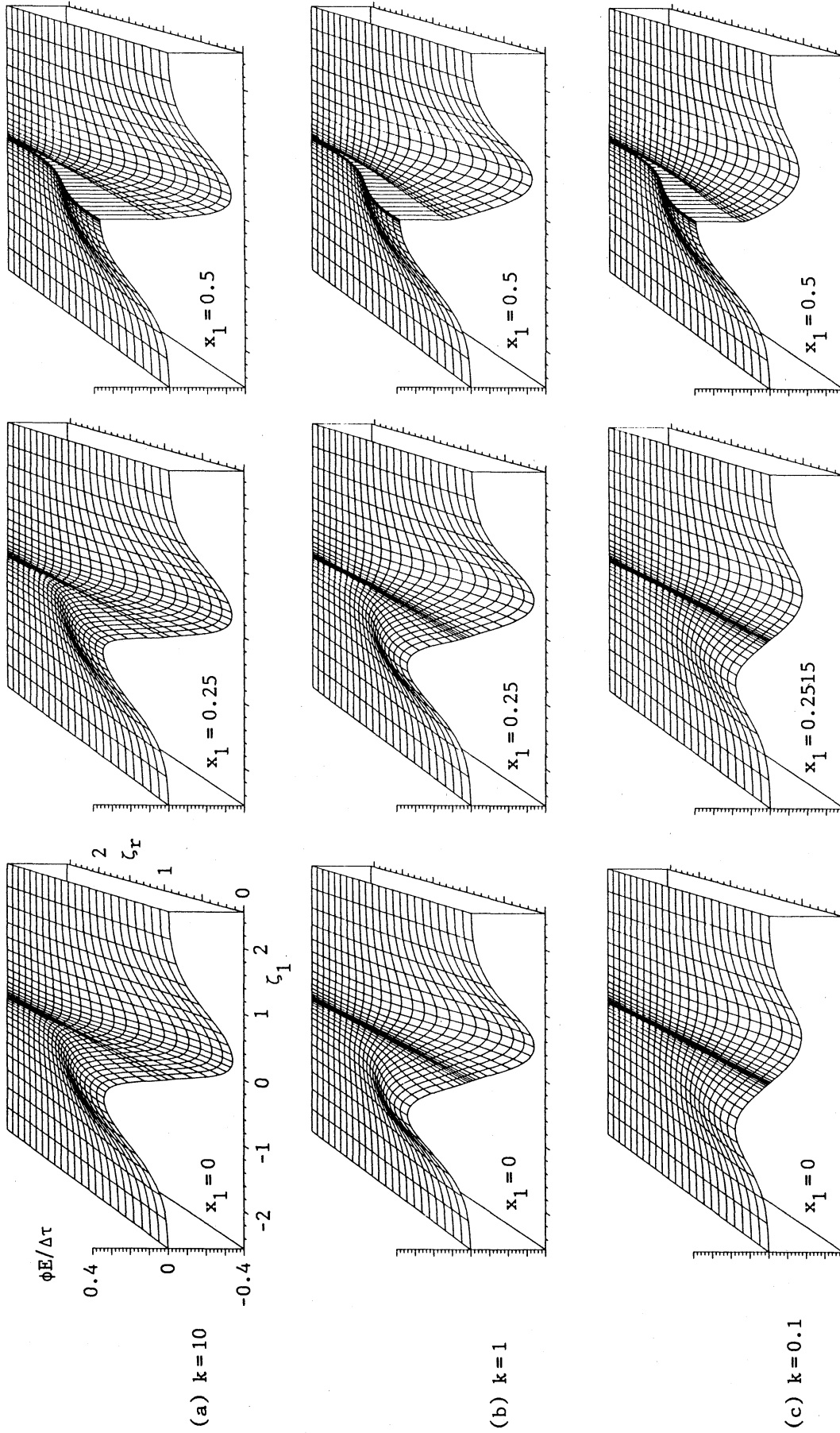


Fig. 5. The velocity distribution function  $\phi E [\beta = \beta_{rQ}; \beta_{rQ} = 4.541 (k=10), 4.644 (k=1), 4.698 (k=0.1)]$ . The scales are common for all the figures. Each three  $\zeta_1 = \text{const}$  and each  $\zeta_r = \text{const}$  lattices in our computation are shown on the surface  $\phi E / \Delta \tau$ . The  $\phi E / \Delta \tau$  is negligibly small at the four corners in the figures, and therefore they may be taken as the reference points.